Journal of Applied Physics

RESEARCH ARTICLE | AUGUST 13 2025

Updates on MURAVES Project at Mt. Vesuvius

Special Collection: Muography: Discoveries, Innovations, and Applications

Yanwen Hong ✉ ; Marwa Al Moussawi; Fabio Ambrosino ; Antonio Anastasio; Samip Basnet; Lorenzo Bonechi; Diletta Borselli ; Alan Bross ; Antonio Caputo; Roberto Ciaranfi; Luigi Cimmino ; Vitaliano Ciulli ; Raffaello D'Alessandro ; Catalin Frosin ; Gabor Nyitrai ; Andrea Giammanco ; Flora Giudicepietro; Sandro Gonzi ; Giovanni Macedonio ; Vincenzo Masone ; Massimo Orazi ; Andrea Paccagnella; Rosario Peluso; Anna Pla-Dalmau; Amrutha Samalan; Giulio Saracino ; Giovanni Scarpato; Paolo Strolin; Michael Tytgat ; Enrico Vertechi

J. Appl. Phys. 138, 064906 (2025)
https://doi.org/10.1063/5.0275078

AIP Publishing

Journal of Applied Physics ARTICLE pubs.aip.org/aip/jap

Updates on MURAVES Project at Mt. Vesuvius

Cite as: J. Appl. Phys. **138**, 064906 (2025); doi: 10.1063/5.0275078
Submitted: 10 April 2025 · Accepted: 22 July 2025 ·
Published Online: 13 August 2025

Yanwen Hong,[1,2,a)] Marwa Al Moussawi,[3,b)] Fabio Ambrosino,[4,5] Antonio Anastasio,[4] Samip Basnet,[3,c)] Lorenzo Bonechi,[6] Diletta Borselli,[6,7] Alan Bross,[8] Antonio Caputo,[9] Roberto Ciaranfi,[6] Luigi Cimmino,[4,5] Vitaliano Ciulli,[6,10] Raffaello D'Alessandro,[10] Catalin Frosin,[6,10] Gabor Nyitrai,[4,5] Andrea Giammanco,[3] Flora Giudicepietro,[9] Sandro Gonzi,[6,10] Giovanni Macedonio,[9] Vincenzo Masone,[4] Massimo Orazi,[9] Andrea Paccagnella,[6,10] Rosario Peluso,[9] Anna Pla-Dalmau,[8] Amrutha Samalan,[2,d)] Giulio Saracino,[4,5] Giovanni Scarpato,[9] Paolo Strolin,[4,5] Michael Tytgat,[1,2] and Enrico Vertechi[9]

AFFILIATIONS

[1]Inter-University Institute for High Energies, Vrije Universiteit Brussel, Brussels 1050, Belgium
[2]Department of Physics and Astronomy, Ghent University, Ghent 9000, Belgium
[3]Centre for Cosmology, Particle Physics and Phenomenology, Université catholique de Louvain, Ottignies-Louvain-la-Neuve 1348, Belgium
[4]National Institute of Nuclear Physics—Section of Naples, Naples 80126, Italy
[5]Department of Physics, University of Naples Federico II, Naples 80126, Italy
[6]National Institute of Nuclear Physics—Section of Florence, Florence 50019, Italy
[7]Department of Physics and Geology, University of Perugia, Perugia 06123, Italy
[8]Fermi National Accelerator Laboratory, Batavia, Illinois 60510, USA
[9]National Institute of Geophysics and Volcanology—Vesuvius Observatory, Naples 80126, Italy
[10]Department of Physics, University of Florence, Florence 50019, Italy

Note: This paper is part of the Special Topic on Muography: Discoveries, Innovations, and Applications.
[a)]**Author to whom correspondence should be addressed:** yanwen.hong@cern.ch
[b)]**Now at:** Muon vision, Inc, Cambridge MA, USA
[c)]**Now at:** Tsung-Dao Lee Institute and School of Physics and Astronomy, Shanghai Jiao Tong University, Shanghai 201210, China
[d)]**Now at:** Paul Scherrer Institute, 5232 Villigen PSI, Switzerland

ABSTRACT

The MUon RAdiography of VESuvius (MURAVES) project aims to employ muography imaging techniques to investigate the internal structure of the summit of Mount Vesuvius, an active volcano located near Naples, Italy. This paper reports recent advancements in data analysis and simulation tools that significantly improve the quality and reliability of the experiment's results. A new track selection method, referred to as the Golden Selection, has been developed to identify high-quality muon tracks by applying an improved χ^2-based criterion. This method enhances the signal-to-background ratio and improves the resolution of the resulting muographic images. Moreover, the simulation framework has been upgraded through the integration of the MULDER (MUon simuLation for DEnsity Reconstruction) library, which consolidates the functionalities of previously used libraries into a single, unified platform. MULDER enables efficient and accurate modeling of muon flux variations induced by topographical features. A good agreement is observed between the simulated and measured muon flux maps, validating the effectiveness of the new analysis and simulation approaches.

I. INTRODUCTION

Mount Vesuvius, located near Naples, Italy, is one of the most hazardous volcanoes due to its history of explosive eruptions and the dense population in its vicinity. Understanding its internal structure is crucial for assessing potential eruption scenarios and implementing effective risk mitigation strategies.[1] Traditional geophysical methods have provided valuable insights but often face limitations in resolution and depth penetration.[2]

Muon radiography, or muography, offers a novel approach by exploiting the natural flux of cosmic-ray muons to probe the internal density distribution of large structures like volcanoes. Muons are highly penetrating particles, making them suitable for imaging geological formations.[3]

The MURAVES project[4,5] aims to apply the muography technique to Mt. Vesuvius to image the internal structure of the summit crater. The experimental setup, located inside a green-colored container on the slope of the crater approximately 1.5 km from the summit, consists of three identical muon trackers (ROSSO, NERO, and BLU), each having a cross-sectional sensitive area of 1 m^2. Every tracker is composed of four XY tracking planes made from plastic scintillators. The X and Y tracking layers are built using 64 plastic scintillator bars per layer, with an isosceles triangular cross-section measuring 3.3 cm at the base and 1.7 cm in height. This design ensures that each muon passes through at least two adjacent bars, allowing for precise position reconstruction. The scintillation light produced by muon interactions is collected via wavelength-shifting (WLS) fibers embedded in the scintillator bars. These fibers guide the light to silicon photomultipliers (SiPMs) for detection. To suppress background from low-energy muons and other particles, a 60 cm thick lead wall is placed between the third and fourth tracking planes in each tracker. This passive shielding increases the energy threshold for detectable muons, effectively filtering out low-energy particles that are more susceptible to multiple scattering and energy loss, which can degrade image resolution. The experiment is currently operational, continuously collecting data from atmospheric cosmic-ray muons.

The following two sections present the recent developments in the MURAVES analysis chain. Section II introduces the *Golden Selection* criteria for track reconstruction, based on χ^2 and designed to enhance data quality of muon tracks. Section III describes the integration of the new MULDER simulation framework, which unifies the modeling of muon transport through the volcanic structure. These two novelties result in a better agreement between experimental and simulated data.

II. DATA ANALYSIS

In the MURAVES experiment, muon track reconstruction is performed using four XY tracking planes within each muon tracker. As a muon traverses a tracker, it generates scintillation light in the plastic scintillator bars, which is subsequently collected by the readout system. These signals are used to determine the hit positions in both the X and Y coordinates across the four tracking planes. By applying a linear fit to the resulting coordinate points, the muon's trajectory is accurately reconstructed, enabling precise analysis of its path through the detector. Further details on the reconstruction algorithm and the complete data analysis chain can be found in the Ph.D. thesis of a collaborator.[6] After track reconstruction, a selection criterion based on the track's χ^2 value, as defined in Eq. (1), is applied to evaluate the quality of the fitted tracks,

$$\chi^2 = \sum_i^n \frac{\left(x_i^{model} - x_i^{data}\right)^2}{\sigma_x^2}. \quad (1)$$

A lower χ^2 value indicates better alignment of the hit clusters, increasing confidence that the reconstructed track corresponds to a genuine muon rather than a random coincidence of noise-induced hits. Random noise can affect the measurement by generating spurious hits that coincide with those produced by an actual muon, introducing ambiguity in the selection of hits used for track reconstruction. The minimum χ^2 criterion is therefore a valuable tool for identifying the most reliable track when multiple candidate tracks are reconstructed within a single event. To this end, a cut on the χ^2 value is applied to select a high-purity subset of tracks, referred to as "golden" tracks, which form the basis of the so-called *Golden Selection*. This selection improves the quality of the resulting muographic images and enhances the accuracy of the density measurements.[7]

In principle, this approach also allows for the identification of multiple muon candidates within the same event, consistent with the possibility of cosmic-ray showers containing two or more muons in close proximity. However, this capability is not currently utilized; at present, only the highest-quality track, defined as the one with the lowest χ^2, is retained for further analysis.

Since the fourth plane of each muon tracker is behind a lead wall, the muon trajectory between third and fourth planes is affected by multiple scattering, and the effect is a function of the muon's momentum as quantified in a previous study.[8] To avoid a bias in the Golden Selection, the χ^2 value is computed using only the first three planes, denoted as χ^2_{3p}. The value estimated with all four planes, denoted as χ^2_{4p}, can be used in future developments of this analysis to roughly classify muon candidates in categories correlated with momentum, with the aim of using this information to improve image quality. The usage of a χ^2-related variable as a proxy for the scattering angle has been already proposed in the literature for a different type of muography apparatus,[9] and in the MURAVES case it is particularly advantageous as the large thickness of the lead wall creates a large uncertainty on the scattering angle,

$$\frac{\Phi_\mu^{Ves}(\Delta\theta, \Delta\phi)}{\Phi_\mu^{Calib}(\Delta\theta, \Delta\phi)} = 1. \quad (2)$$

The current strategy relies on the assumption that the muon flux measured from open-sky directions above Mt. Vesuvius should be consistent with the flux measured during calibration runs, i.e., under free-sky conditions—along the corresponding directions. To validate this, a control region, shown in Fig. 1, is defined. This region is selected to lie sufficiently far from the contours of the volcano in order to minimize systematic effects due to scattering or absorption near the structure's edges. Within this control region, the following condition is expected to hold between the muon fluxes measured in the Vesuvius data sets and those obtained from free-sky data sets:

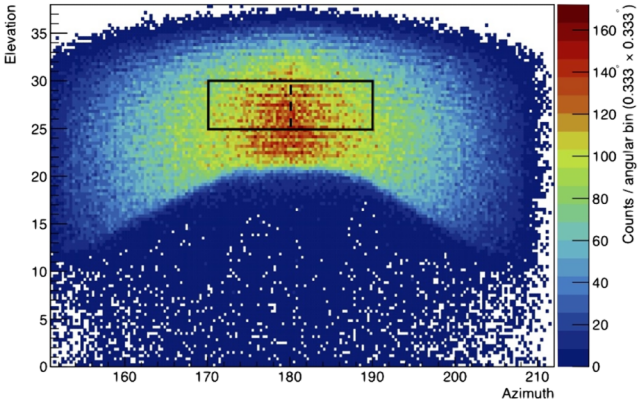

(a)

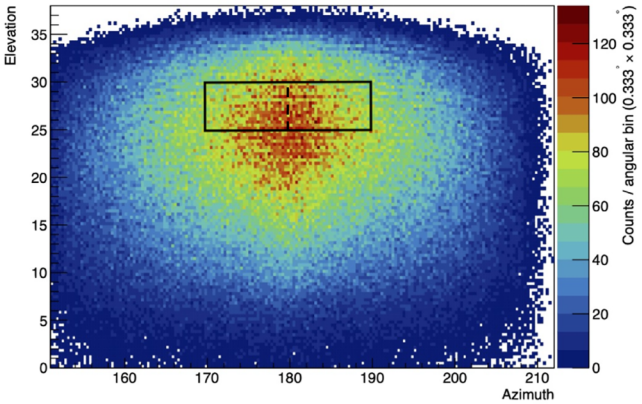

(b)

FIG. 1. Control regions shown in the $\theta - \phi$ flux map, using NERO detector data. (a) Control region (highlighted by the black box) defined within the Vesuvius data set, selected to represent open-sky directions for flux comparison. (b) Control region (highlighted by the black box) defined within the free-sky data set, selected to represent open-sky directions for flux comparison.

Based on the condition defined in Eq. (2), independent χ^2_{3p} cuts are applied to both the Vesuvius and free-sky data sets. The combination of these cuts, i.e., the pair of χ^2_{3p} thresholds for the Vesuvius and free-sky data that satisfy the condition, using NERO detector data as an example, is illustrated in Fig. 2.

The selected combination of χ^2_{3p} cuts is now used to evaluate the time-normalized muon transmission through the *Vesuvius Region*, defined by the angular intervals $\phi \in [170°, 190°]$ and $\theta \in [12°, 18°]$. The effective ratio between the measured and calibration fluxes, referred to as the transmission $T(\theta, \phi)$, accounts for and largely cancels out detector-related effects. It is calculated using the following expression:

$$T(\theta, \phi) = C \cdot \frac{N_{mes}(\theta, \phi)}{N_{cal}(\theta, \phi)}, \tag{3}$$

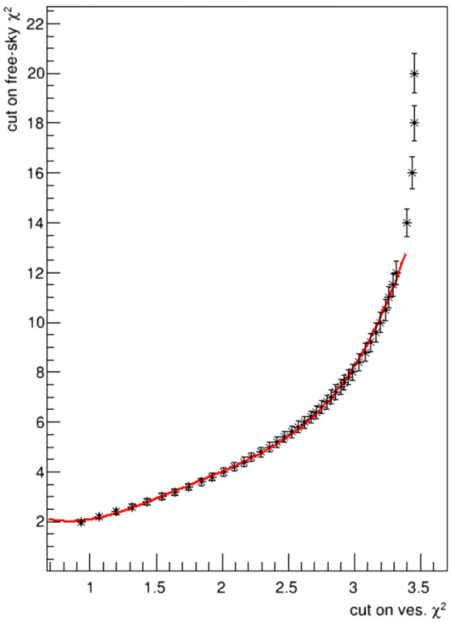

FIG. 2. The χ^2_{3p} combination on the Vesuvius and free-sky data sets satisfying the condition defined in Eq. (2) in the control region, using NERO detector working point 15 data.

where $N_{mes}(\theta, \phi)$ and $N_{cal}(\theta, \phi)$ represent the angular distributions of muon counts from the Vesuvius and calibration data sets, respectively, and C is a normalization constant. The measured transmission in the Vesuvius region for all data sets is shown in Fig. 3, as a function of χ^2_{3p} threshold on Vesuvius data sets. A common upper cut on χ^2_{3p} was applied across all detectors and operation temperature of silicon photomultipliers (SiPMs), namely, working points (WPs), set to a value of 3.2 (indicated by the green line in the figure). This threshold was chosen based on the plateau region highlighted by the blue band, which indicates stability in the transmission values.

However, due to differences between the Vesuvius and calibration data sets, including acquisition periods, environmental conditions, and detector operating states, the optimal free-sky χ^2_{3p}

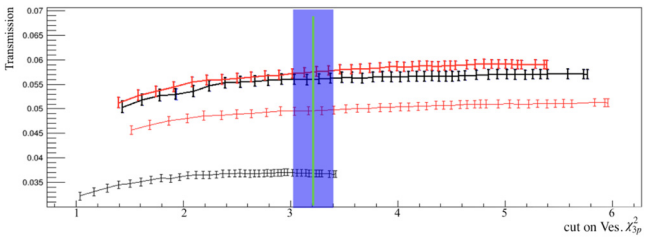

FIG. 3. Measured transmission as a function of the maximum χ^2_{3p} cut value in the Vesuvius region. The black and red curves represent NERO and ROSSO data sets, with bold representing WP20 and normal, WP15.

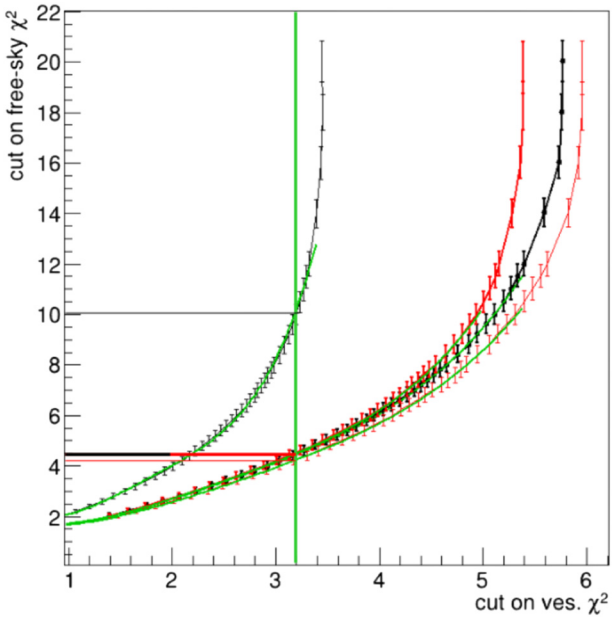

FIG. 4. The χ^2_{3p} combination on the Vesuvius and the free-sky data sets satisfying the condition defined in Eq. (2) for all available data sets. The black and red curves represent NERO and ROSSO data sets, with bold and normal representing WP20 and WP15, respectively.

thresholds are not identical across all data sets. Based on the fixed cut value of 3.2 applied to the Vesuvius data sets, the corresponding optimal χ^2_{3p} cut values for the free-sky data sets were determined from the cut combination analysis shown in Fig. 4. The resulting values are 10.0 for NERO WP15, 4.5 for NERO WP20, 4.3 for ROSSO WP15, and 4.5 for ROSSO WP20.

A general challenge in muographic applications to volcanology arises from the substantial attenuation of the muon flux when traversing rock layers several thousand meters thick. To mitigate this limitation, our study focuses on the summit cone of Mount Vesuvius, where the typical rock thickness is less than 1200 m. The

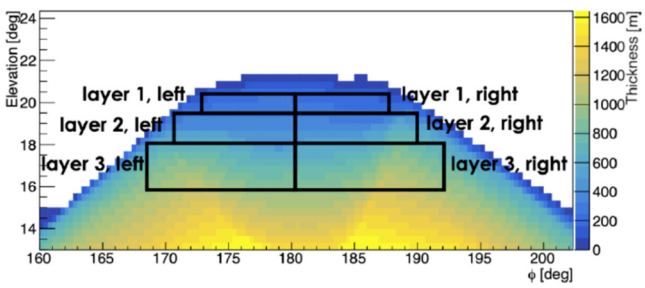

FIG. 5. The rock thickness map of Mt. Vesuvius summit crater observed in MURAVES experiment location, and the angular regions (in bold black boxes) used for the study.

TABLE I. $\theta - \phi$ regions used in the left-right asymmetry study.

Elevation $\Delta\theta$	Left ($\Delta\phi$)	Right ($\Delta\phi$)
$\text{Top}_{(\text{layer1})}$ [19.5°–20.5°]	[173.0°–180.0°]	[180.0°–187.0°]
$\text{Middle}_{(\text{layer2})}$ [18.0°–19.5°]	[170.0°–180.0°]	[180.0°–190.0°]
$\text{Bottom}_{(\text{layer3})}$ [16.0°–18.0°]	[168.0°–180.0°]	[180.0°–192.0°]

θ–ϕ angular regions selected for this study are shown in Fig. 5. These regions span three layers of elevation angles chosen across the summit cone and are divided into left and right azimuthal sectors to enable the investigation of possible left-right asymmetries. The specific angular intervals used in the analysis are detailed in Table I.

Table II presents the measured transmission values in the left and right regions of Mount Vesuvius, evaluated across three elevation layers, before and after applying the updated χ^2_{3p} cut criterion. As expected, transmission increases with elevation angle, that is, higher values are observed in the top layer compared to the bottom, due to the decreasing rock thickness toward the summit.

Across all angular bins, the ROSSO detector consistently reports higher transmission values than the NERO detector. In the top layer, transmission on the right side is generally greater than on the left across all data sets, with the exception of NERO WP20. Conversely, in the middle and bottom layers, this trend reverses, with left-sided angular bins typically exhibiting higher transmission than those on the right. Overall, based on these transmission measurements, no clear left–right asymmetry is observed in the summit crater region.

TABLE II. Measured muon transmission values in the left and right angular regions of Mount Vesuvius, evaluated across three elevation layers. Results are shown before and after applying the updated χ^2_{3p} track selection criterion.

	No cuts		New χ^2_{3p} cut	
Data sets	T_{left}	T_{right}	T_{left}	T_{right}
		Top		
ROSSO WP15°C	0.329	0.336	0.300	0.307
ROSSO WP20°C	0.344	0.348	0.308	0.315
NERO WP15°C	0.302	0.336	0.232	0.239
NERO WP20°C	0.284	0.348	0.259	0.259
		Middle		
ROSSO WP15°C	0.147	0.161	0.132	0.142
ROSSO WP20°C	0.168	0.160	0.144	0.139
NERO WP15°C	0.153	0.149	0.118	0.112
NERO WP20°C	0.155	0.150	0.136	0.129
		Bottom		
ROSSO WP15°C	0.080	0.083	0.069	0.072
ROSSO WP20°C	0.087	0.090	0.074	0.076
NERO WP15°C	0.072	0.075	0.055	0.058
NERO WP20°C	0.085	0.084	0.072	0.071

III. MUON FLUX SIMULATION

Accurate simulations are crucial for interpreting muographic data and modeling muon propagation through the complex geological structure of Mount Vesuvius. To support data analysis, the MURAVES experiment has developed a comprehensive simulation workflow. This includes the generation of cosmic-ray showers using tools such as CORSIKA,[10] CRY,[11] and EcoMug,[12] which we compared in Ref. 8, as well as muon transport through rock using Monte Carlo simulators like PUMAS,[13] TURTLE,[14] and MUSIC.[15] The detector response is modeled using Geant4.[16] The integration of these tools enables the optimization of track reconstruction algorithms and provides more accurate estimates of background contributions.

In our previous simulation framework, we used the TURTLE[14] (Transport of Uncharged Particles Through Matter) program in conjunction with PUMAS[13] (Parallel Ultra-fast MUon and Tau Neutrino Simulator) to incorporate the topography of the Mount Vesuvius region and model muon transport through the mountain. The application of these tools was described in detail in previous publication.[17] We now adopt a unified framework called MULDER (MUon simuLation for DEnsity Reconstruction),[18] which integrates the functionalities of both TURTLE and PUMAS into a single utility library. MULDER is designed to compute local variations in the atmospheric muon flux induced by geophysical features using a Digital Elevation Model (DEM). In our specific application, we utilize a 5 m-resolution DEM of the Mt. Vesuvius region, provided by the INGV (National Institute of Geophysics and Volcanology, Italy), with the precise geographic coordinates of the MURAVES muon tracker defining the local position. Mulder uses a parametric model as reference muon flux,[19] and the input energy spectrum used in our case spans a log-uniform distribution from 3 to 10 000 GeV. This integration minimizes cumulative errors arising from disparate tools, as well as provides enhanced computational efficiency.

The latest simulation results obtained using the MULDER framework are shown in Fig. 6(a), while Fig. 6(b) presents the corresponding experimental data from the NERO detector at a working point of 15°, collected over 948.2 h. The reduced flux observed at the

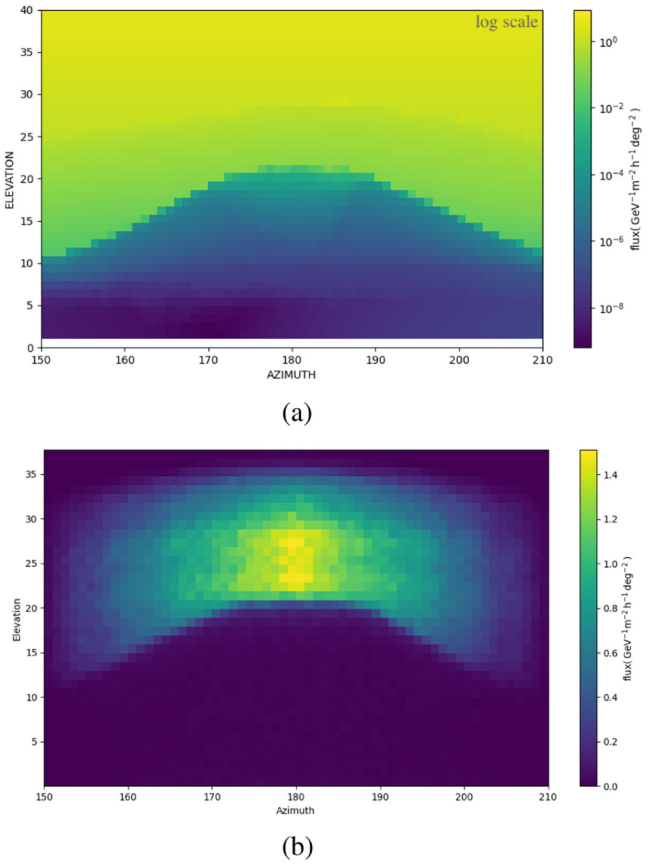

FIG. 6. Comparison between simulated and experimental muon flux maps. (a) Simulated muon flux map generated using the MULDER framework, presented on a log scale. Detector geometric acceptance has not been accounted for in this simulation. (b) Measured muon flux map from the NERO detector.

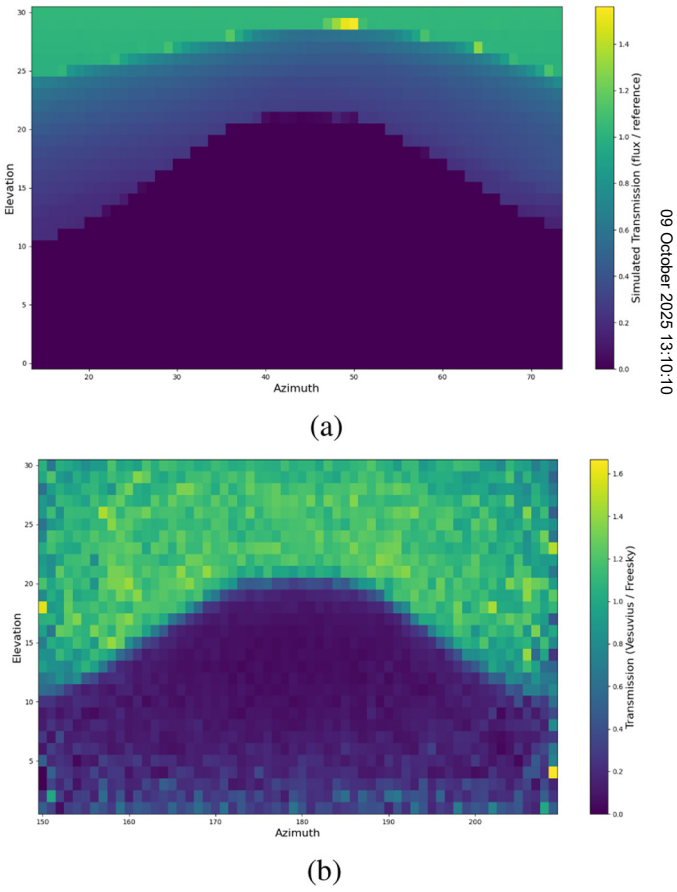

FIG. 7. Comparison between simulated and experimental transmission maps. (a) Simulated transmission generated using the MULDER framework. (b) Measured transmission map from the ROSSO detector, based on 1143.3 h of data at a working point of 15°.

edges of the field of view is attributed to the limited geometric acceptance of the detector's active area. In this case, detector acceptance effects have not been included in the MULDER simulation. Nonetheless, the observed order of magnitude agreement between the simulated and measured flux maps demonstrates the initial effectiveness of both the Golden Selection criteria and the MULDER framework. In order to mitigate detector induced effects, transmission maps are also generated. It is defined as the ratio of the muon flux traversing the object to the reference or open-sky flux. Figure 7(a) presents the simulated transmission map derived from the modeled flux through Vesuvius crater relative to the local reference flux, while Fig. 7(b) shows the transmission obtained by comparing ROSSO detector data to open-sky flux measurements. Both maps exhibit a consistent pattern, indicating the agreement between simulation and observation. To further quantify this agreement, a systematic comparison within both the Control Region and the Vesuvius Region is essential. This next step will further allow evaluation of the reconstruction accuracy, validation of the Golden Selection criteria, and refinement of the MULDER framework.

This consistency enhances confidence in the muographic reconstruction and provides deeper insights into the internal structure of Mount Vesuvius. Ongoing studies are focused on refining transmission comparisons and improving density extraction techniques to further enhance reconstruction accuracy.

IV. CONCLUSION

The MURAVES experiment at Mt. Vesuvius has achieved advancements in both data analysis and simulation frameworks for muographic imaging. The implementation of the Golden Selection, a refined track quality criterion based on the χ^2 value calculated from the first three detector planes, has led to a cleaner and more reliable sample of reconstructed muon tracks. This enhancement directly improves the resolution and accuracy of muographic images, enabling more precise density measurements of the volcanic structure. In parallel, the deployment of the unified MULDER simulation framework has substantially improved our ability to model muon propagation through the complex topography of Mt. Vesuvius. The new framework provides a more streamlined and computationally efficient approach to simulating atmospheric muon fluxes. Ongoing studies are focused on detailed transmission comparisons and precise density extraction techniques to further improve the accuracy of density reconstructions. These efforts aim to advance our understanding of the internal structure of Mt. Vesuvius summit crater and contribute to more reliable volcanic hazard assessment and risk mitigation strategies.

ACKNOWLEDGMENTS

This work was partially supported by the Fonds de la Recherche Scientifique—FNRS under Grant No. T.0129.25 and the Fonds Wetenschappelijk Onderzoek—Vlaanderen (FWO) under Grant No. G0AR825N.

AUTHOR DECLARATIONS

Conflict of Interest

The authors have no conflicts to disclose.

Author Contributions

Yanwen Hong: Formal analysis (equal); Investigation (equal); Software (equal); Writing – original draft (lead); Writing – review & editing (equal). **Marwa Al Moussawi:** Formal analysis (equal); Investigation (equal); Software (equal). **Fabio Ambrosino:** Conceptualization (equal). **Antonio Anastasio:** Conceptualization (equal). **Samip Basnet:** Formal analysis (lead); Investigation (equal); Software (equal). **Lorenzo Bonechi:** Resources (equal). **Diletta Borselli:** Writing – review & editing (supporting). **Alan Bross:** Resources (equal). **Antonio Caputo:** Resources (equal). **Roberto Ciaranfi:** Conceptualization (equal); Methodology (equal). **Luigi Cimmino:** Conceptualization (equal); Data curation (equal); Investigation (equal); Methodology (equal); Supervision (equal). **Vitaliano Ciulli:** Conceptualization (equal). **Raffaello D'Alessandro:** Conceptualization (equal). **Catalin Frosin:** Writing – review & editing (supporting). **Gabor Nyitrai:** Writing – review & editing (supporting). **Andrea Giammanco:** Funding acquisition (equal); Supervision (lead); Writing – review & editing (lead). **Flora Giudicepietro:** Resources (lead). **Sandro Gonzi:** Writing – review & editing (supporting). **Giovanni Macedonio:** Resources (lead). **Vincenzo Masone:** Conceptualization (equal). **Massimo Orazi:** Resources (equal). **Andrea Paccagnella:** Writing – review & editing (supporting). **Rosario Peluso:** Resources (equal). **Anna Pla-Dalmau:** Resources (supporting). **Amrutha Samalan:** Formal analysis (equal); Investigation (equal); Software (equal). **Giulio Saracino:** Conceptualization (lead); Funding acquisition (lead); Project administration (lead); Supervision (equal). **Giovanni Scarpato:** Resources (equal). **Paolo Strolin:** Conceptualization (equal). **Michael Tytgat:** Conceptualization (equal); Funding acquisition (equal); Methodology (equal); Resources (equal); Supervision (lead); Writing – review & editing (lead). **Enrico Vertechi:** Resources (equal).

DATA AVAILABILITY

The data that support the findings of this study are available from the corresponding author upon reasonable request.

REFERENCES

[1]G. De Natale, C. Troise, and R. Somma, "Invited perspectives: The volcanoes of Naples: How can the highest volcanic risk in the world be effectively mitigated? Nat. Haz. Earth Syst. Sci. **20**, 2037–2053 (2020).
[2]N. Linde, T. Ricci, L. Baron, A. Shakas, and G. Berrino, "The 3-D structure of the Somma-Vesuvius volcanic complex (Italy) inferred from new and historic gravimetric data," Sci. Rep. **7**, 8434 (2017).
[3]H. K. Tanaka *et al.*, "Muography," Nat. Rev. Methods Primers **3**, 88 (2023).
[4]R. D'Alessandro, F. Ambrosino, G. Baccani, L. Bonechi, M. Bongi, A. Caputo, R. Ciaranfi, L. Cimmino, V. Ciulli, M. D'Errico *et al.*, "Volcanoes in Italy and the role of muon radiography," Philos. Trans. R. Soc. A **377**, 20180050 (2019).
[5]G. Saracino *et al.*, "The MURAVES muon telescope: Technology and expected performances," Ann. Geophys. **60**, S0103 (2017).
[6]M. D'Errico, "Muon radiography applications: The study of the Mt. Vesuvius Great Cone and the search and 3D modeling of underground cavities," Ph.D. thesis (Università degli studi di Napoli Federico II, 2021).
[7]S. Basnet, "Muography: Development of a portable detector and analysis of the MURAVES data," Ph.D. thesis (Louvain University, 2024).

[8]M. Moussawi, S. Basnet, L. Bonechi, L. Cimmino, R. DÁlessandro, M. DÉrrico, A. Giammanco, R. Karnam, G. Macedonio, C. Rendon *et al.*, "The simulations chain of the MURAVES experiment," arXiv:2202.03375 (2022).
[9]S. Vanini, P. Calvini, P. Checchia, A. Rigoni Garola, J. Klinger, G. Zumerle, G. Bonomi, A. Donzella, and A. Zenoni, "Muography of different structures using muon scattering and absorption algorithms," Philos. Trans. R. Soc. A **377**, 20180051 (2019).
[10]D. Heck *et al.*, "CORSIKA: A Monte Carlo Code to simulate extensive air showers," Technical Report FZKA 6019 (Forschungszentrum Karlsruhe, 1998).
[11]C. Hagmann, D. Lange, and D. Wright, "Cosmic-ray shower generator (CRY) for Monte Carlo transport codes," in *2007 IEEE Nuclear Science Symposium Conference Record* (IEEE, 2007), Vol. 2, pp. 1143–1146.
[12]D. Pagano, G. Bonomi, A. Donzella, A. Zenoni, G. Zumerle, and N. Zurlo, "EcoMug: An efficient COsmic MUon generator for cosmic-ray muon applications," Nucl. Instrum. Method A **1014**, 165732 (2021).
[13]V. Niess, A. Barnoud, C. Cârloganu, and E. Le Ménédeu, "Backward Monte-Carlo applied to muon transport," Comput. Phys. Commun. **229**, 54 (2018).
[14]V. Niess, A. Barnoud, C. Cârloganu, and O. Martineau-Huynh, "TURTLE: A C library for an optimistic stepping through a topography," Comp. Phys. Commun. **247**, 106952 (2020).
[15]P. Antonioli *et al.*, "A three-dimensional code for muon propagation through the rock: MUSIC," Astropart. Phys. **7**, 357 (1997).
[16]S. Agostinelli *et al.*, "GEANT4—A simulation toolkit," Nucl. Instrum. Methods A **506**, 250 (2003).
[17]A. Giammanco Y. Hong (MURAVES), "Simulation tools, first results, and experimental status of the MURAVES experiment," arXiv:2311.13663 (2024).
[18]See https://github.com/niess/mulder for MULDER program source files.
[19]M. Guan, M.-C. Chu, J. Cao, K.-B. Luk, and C. Yang, "A parametrization of the cosmic-ray muon flux at sea-level," arXiv:1509.06176 [hep-ex] (2015).